Dynamic wetting property investigation of AFM tips in micro/nanoscale

The wetting properties of AFM probe tips are of concern in AFM tip related force measurement, fabrication, and manipulation techniques, such as “dip-pen” nanolithography, nano-dispensing, micro/nanomanipulation, and nanotribological investigation, and even basic imaging. In these applications, the meniscus force often dominates the adhesion force. As a result, the wetting properties of cantilever tips play crucial roles in these operations and may introduce artifacts into the measurement results. Due to their geometrical complexity and extremely small size, there is no direct measurement for AFM tip wetting properties. In this study, a novel method is proposed to directly measure AFM tip wetting properties at the nanoscale based on the micro-Wilhelmy balance method. The dynamic contact angles of AFM tips are obtained through capillary force measurement during extension and retraction motion of the AFM tips relative to nanobubbles using the nano-Wilhelmy balance method.

To employ the nano-Wilhelmy balance method to AFM tips, the capillary force and the three phase contact lines need to be accurately measured during tip-nanobubble interaction. In this study, the capillary force measurement is achieved through tip-bubble interaction, as shown in **Fig 1**. The whole interaction is divided into two regions: pyramidal interaction region and spherical interaction region. Then the vertical forces applied on AFM tips can be given as:

$$F_{vert} = \sum_{i=1}^{4} \gamma_{LV} \tau_i h(z) \cos(\beta_i + \theta) \tag{1}$$

where γ_{LV} is the liquid vapor surface tension of water, θ is the contact angle, m_i is the length of the three phase contact line on the ith (i = 1, 2, 3, and 4) side wall of the tip, τ_i is constant for ith side wall of the tip, h (z) is indentation depth and β_i is the angle of the side wall relative to the vertical direction.

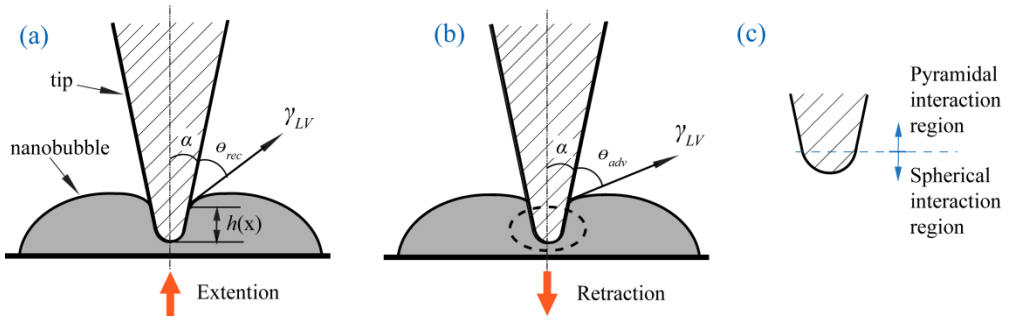

Fig 1. Schematic of AFM tip-nanobubble interaction during extension (a) and retraction (b) of the AFM scanner. The interaction is divided into two regions, spherical interaction region and pyramidal interaction region (c).

In the pyramidal interaction region, the surface tension length varies linearly with indentation depth; and the coefficient τ_i can be measured with much higher accuracy. Given θ, β_i, and γ_{LV} are constant, the vertical force applied to AFM tips during extension motion is different from that of the retraction motion due to the existence of contact angle hysteresis. We have:

$$\frac{dF_{vert}^{adv}}{dh(z)} = \sum_{i=1}^{4} \gamma_{LV} \tau_i \cos(\beta_i + \theta_{adv}) \tag{2}$$

and

$$\frac{dF_{vert}^{rec}}{dh(z)} = \sum_{i=1}^{4} \gamma_{LV} \tau_i \cos(\beta_i + \theta_{rec}) . \tag{3}$$

where θ_{adv} and θ_{rec} are the advancing and receding contact angles, respectively.

From **Eq. (2)** and **Eq. (3)**, one can expect that during both extension and retraction motion of the AFM scanner, the capillary force should linearly increase with indentation depth. Since θ_{adv} is larger than θ_{rec}, $dF_{vert}^{adv}/dh\,(z)$ should be smaller than $dF_{vert}^{rec}/dh\,(z)$. Moreover, the dynamic contact angles θ_{adv} and θ_{rec} can be obtained by recording the capillary force during tip-nanobubble interaction.

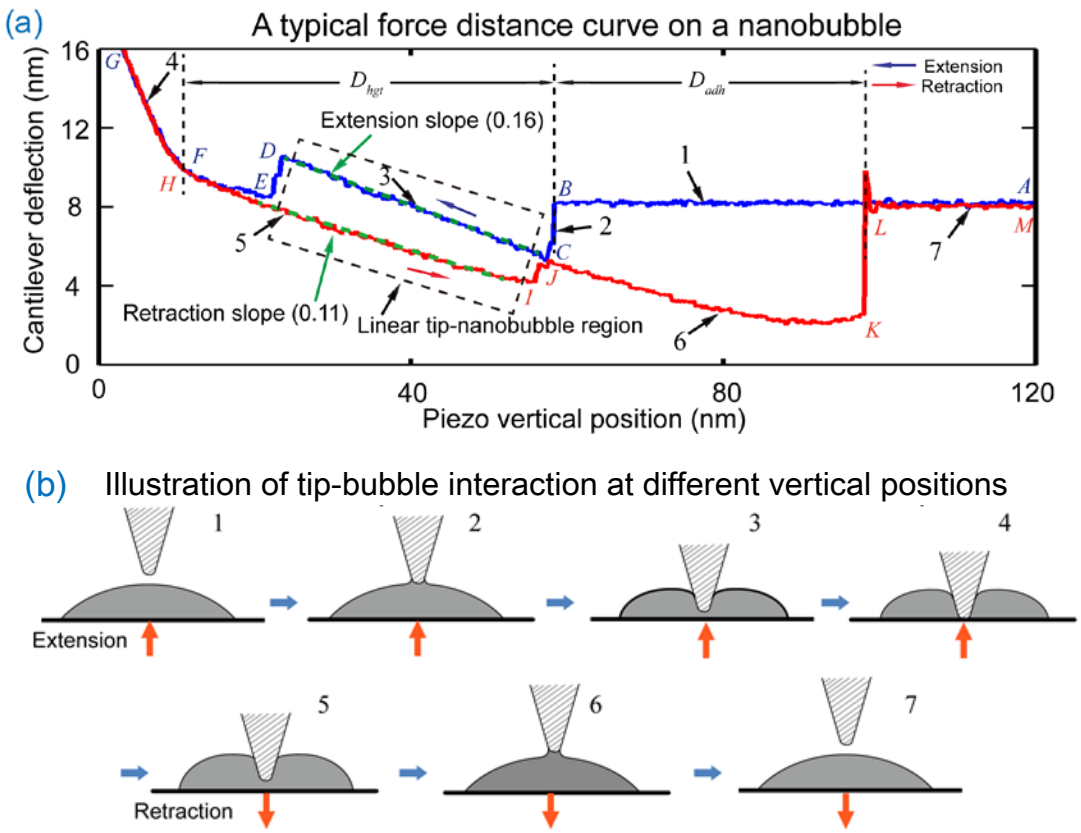

Fig 2. Tip-nanobubble interaction. (a) A typical force distance curve measured on a nanobubble. The whole process is divided into seven sections. (b) Illustration of the seven sections. The force distance curve clearly shows the pyramidal interaction region.

A typical force distance curve obtained on a nanobubble is shown in **Fig 2a**. The whole tip-nanobubble interaction can be divided into seven sections (**Fig 2b**). In the extension motion of the AFM scanner, the tip approaches the nanobubble. Before the tip gets contact with the nanobubble, there is no interaction force between them (points A→B). At point B, the AFM tip contacts the nanobubble, and a meniscus bridge forms between the tip and the nanobubble. The tip is rapidly drawn into the nanobubble due to the capillary force (points B→C), entering the pyramidal tip-nanobubble interaction region. The force linearly increases with decreasing piezo vertical position (points C→D). After point D, the tip is first attracted to the sample surface due to electrostatic forces and Van der Waals forces. Then, the tip contacts the solid sample surface, resulting in a rapid linear increase of cantilever deflection (F→G).

In the retraction motion, the tip reenters the pyramidal tip-nanobubble interaction region (H→I). This is a result of decreasing length of the three phase contact line and decreasing interaction force. During retraction, the contact angle is an advancing contact angle. The observed slope of cantilever deflection v.s. piezo vertical position in section 5 is lower than that in section 3, which is consistent with the derived mathematic model given in **Eq. (2)** and **(3)**.

At point I, the AFM tip enters the spherical contact region (J→K). In this section, the three phase contact line retreats from the boundary between the pyramidal and spherical regions, entering the spherical region, until the meniscus breaks and the cantilever deflection rapidly goes to zero (L→M). Two other parameters can be extracted from **Fig 2**. The distance D_{hgt}, the height of the nanobubble, is the vertical displacement the scanner travels from point B to point F (or H). The distance D_{adh}, the vertical distance between points B and L, is related to the maximum adhesive force between the cantilever tip and the nanobubble.

Force volume mode scanning is used. In the force volume mode, the AFM cantilevers scan sample surfaces with fixed step sizes along *x* and *y* axes. The result is shown in **Fig 3**. It shows that D_{hgt} increases with nanobubble height, following the profile of the nanobubble. D_{adh} inversely changes with nanobubble height. With the force-distance curves over nanobubble surfaces, the dynamic contact angles for each AFM probe can be obtained with force distance curves obtained near the nanobubble apex using **Eqs. (2)** and **(3)**. The advancing contact angle θ_{adv} and receding contact angle θ_{rec} for the silicon cantilever (RFESP) are 61.8±1.6° and 44.3±0.7°, respectively. For the silicon nitride cantilever (ORC8), the calculated values of θ_{adv} and θ_{rec} are 46.3±1.1° and 42.0±0.7°, respectively.

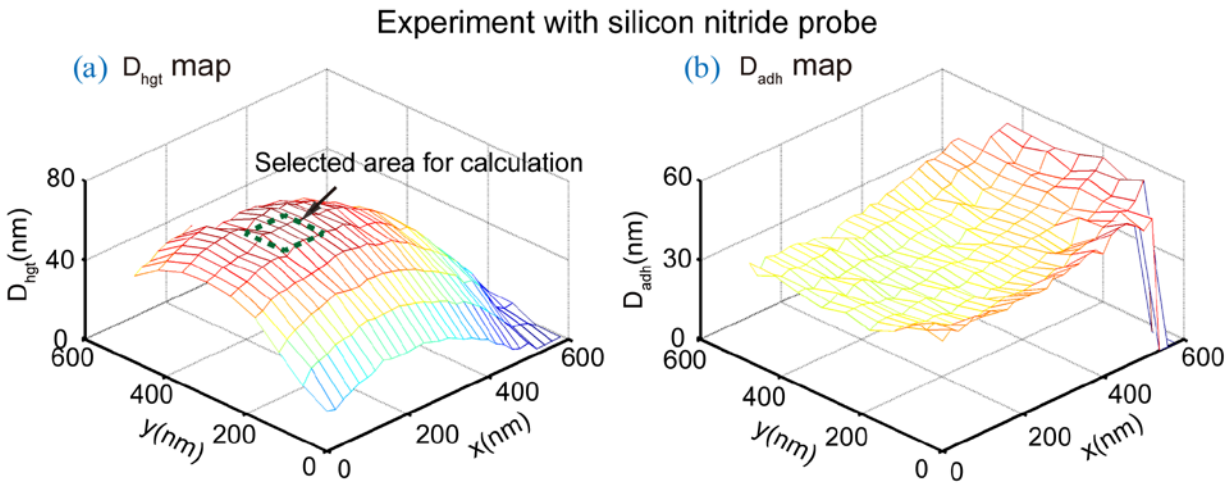

Fig 3. Constructed maps of D_{hgt} (a) and D_{adh} (b) with force volume measurement of force distance curves.

Yuliang Wang, associate professor, school of mechanical engineering and automation, Beihang University, E-mail: wangyuliang@buaa.edu.cn

References

[1] Yuliang Wang*, Huimin Wang, Shusheng Bi, and Bin Guo, Nano-Wilhelmy investigation of dynamic wetting properties of AFM tips through tip-nanobubble interaction. Scientific Reports, 2016, 6:30021.

[2] Dayong Li, Yuliang Wang*, Yunlu Pan, Xuezeng Zhao Measurements of slip length for flows over graphite surface with gas domains, Applied Physics Letters, 2016, 109:151602.

[3] Yuliang Wang*, Xiaolai Li, Shusheng Bi, Xiaofeng Zhu, and Jinhua Liu, 3D micro-particle image modeling and its application in measurement resolution investigation for visual sensing based axial localization in an optical microscope, Measurement Science and Technology, In press.